

Voronoi Diagrams for Parallel Halflines in 3D

Franz Aurenhammer*

Günter Paulini†

Bert Jüttler‡

Abstract

We consider the Euclidean Voronoi diagram for a set of n parallel halflines in \mathbb{R}^3 . A relation of this diagram to planar power diagrams is shown, and is used to analyze its geometric and topological properties. Moreover, a simple plane-sweep algorithm is given that computes the Voronoi diagram for parallel halflines at logarithmic cost per face.

1 Introduction

The Voronoi diagram is a powerful and widely used geometric partitioning structure. Many of its properties are well understood, also in generalized settings of various kinds; see e.g. [5].

Still, knowledge becomes quite sparse in dimensions larger than two, when sites of more general shape are allowed. This concerns the structural as well as the algorithmic properties, and is already true for the generalization from point sites to line segments. The combinatorial complexity of the Voronoi diagram for n line segments, and in particular, for n straight lines in Euclidean d -space \mathbb{R}^d can be as large as $\Omega(n^{d-1})$; see [3]. The only known upper bound follows from a general result on lower envelopes of hypersurfaces [12], and is $O(n^{d+\varepsilon})$ for any $\varepsilon > 0$.

Even in \mathbb{R}^3 , no better bounds than $\Omega(n^2)$ and $O(n^{3+\varepsilon})$, respectively, are known up to date. This may be partially due to the complicated shape of the arising bisector surfaces. They contain, among other components, parabolic and hyperbolic patches, and can lead to a diagram of fairly complicated topological structure. Already for three straight lines as sites, the induced structure gets so intricate that a separate paper has been devoted to its exploration [8].

To make the problem more tractable, several restricted scenarios have been considered. For example, if the line segment sites are confined to have constantly many orientations [10], then the size of the diagram reduces to $O(n^{2+\varepsilon})$. If, on the other hand, the underlying distance function is polyhedral

and convex, then the diagram becomes piecewise-linear. The upper bound then can be tightened to $O(n^2 \alpha(n) \log n)$, even when constant-sized convex polyhedra are allowed as sites; see [6] and [9], respectively. A practical algorithm for computing the medial axis of a nonconvex polytope in \mathbb{R}^3 under a convex polyhedral distance function is given in [2].

In the present note, we discuss a simple though non-trivial special case for the Euclidean distance, namely, the case where all sites are parallel halflines in \mathbb{R}^3 , being unbounded in the same direction. Apart from the theoretical interest, practical applications arise in certain problems in the drilling industry (mining exploitation, offshore drilling, hydraulics, etc.), as is reported by Adamou [1]. In particular, such Voronoi diagrams serve in the exploration of the nearest layers to avoid collision between wells and identifying unwanted plies. A related problem where this diagram may be useful is approximate nearest-neighbor searching among a set of parallel line segments in \mathbb{R}^3 , which has been studied in Emiris et al. [7].

As an interesting fact, the Voronoi diagram for parallel halflines is related to planar power diagrams. We describe this correspondence in Section 2, along with its structural implications. On the algorithmic side, a simple plane-sweep algorithm is obtained in Section 3. Basically, a power diagram for fixed sites has to be updated under continuous changes of site weights. Section 4 studies the behavior of the trisector curves for the halfline Voronoi diagram, motivated by an attempt to reduce the $O(n^{2+\varepsilon})$ upper bound on its combinatorial complexity (which follows from the result in [10]) to $O(n^2)$. Some extensions of our results are mentioned in Section 5.

2 Diagram

Let $H = \{h_1, \dots, h_n\}$ be a set of parallel halflines in \mathbb{R}^3 . We assume that each h_i is vertical, and unbounded in negative z -direction. The upper endpoint of h_i is denoted by z_i . We call z_i the *tip* of h_i , and (by slight abuse of notation) we will use z_i also to denote the z -coordinate of the tip. The distance of a point $x \in \mathbb{R}^3$ to a halfline h_i is defined as

$$d(x, h_i) = \min\{\delta(x, q) \mid q \in h_i\}$$

where δ denotes the Euclidean distance function. This distance is the normal distance of x to the supporting

*Institute for Theoretical Computer Science, University of Technology, Graz, Austria, auren@igi.tugraz.at

†Institute for Theoretical Computer Science, University of Technology, Graz, Austria, guenter.paulini@igi.tugraz.at

‡Institute of Applied Geometry, Johannes Kepler University, Linz, Austria, bert.juettler@jku.at

line, ℓ_i , of h_i , unless $d(x, h_i)$ is attained at the tip z_i . The region of a halfline in the Voronoi diagram, $\mathcal{V}(H)$, of H is given by

$$\text{reg}(h_i) = \{x \in \mathbb{R}^3 \mid d(x, h_i) \leq d(x, h_j), \text{ for all } j\}.$$

Regions are bounded by bisectors, B_{ij} , for pairs of halflines h_i, h_j . Let the respective tips satisfy $z_i \geq z_j$. Then B_{ij} is composed of three parts: A planar patch, contained in the (vertical) bisecting plane of the lines ℓ_i and ℓ_j , a piece of a parabolic cylinder equidistant from line ℓ_i and point z_j , and another planar patch in the bisecting plane of the points z_i and z_j . In the case $z_i = z_j$, B_{ij} is a single vertical plane.

The analysis of the structure of $\mathcal{V}(H)$ is eased by the fact that the generators of the parabolic patches are horizontal lines. This gives the following property:

Observation 1 *The intersection of B_{ij} with any horizontal plane is a straight line.*

Denote with E^Δ the horizontal plane $z = \Delta$, and consider the lines $b_{ij} = B_{ij} \cap E^\Delta$. As bisectors intersect 3 by 3 in trisectors $t_{ijk} = B_{ij} \cap B_{ik} \cap B_{jk}$, the lines b_{ij} , b_{ik} , and b_{jk} concur in a common point (or are parallel), for any pairwise different indices i, j, k . This implies, by a result in [4], that the line system $(b_{ij})_{1 \leq i < j \leq n}$ is the set of *power lines* defined by n weighted points in E^Δ . A more direct argument follows from the lemma below.

Lemma 1 *Consider the point $p_i = \ell_i \cap E^\Delta$, and assign the weight $w_i = -\max\{0, (\Delta - z_i)\}^2$ to it. For any $x \in E^\Delta$, we have $d(x, h_i)^2 = \delta(x, p_i)^2 - w_i$.*

Proof. If E^Δ lie below z_i then $p_i \in h_i$ and $w_i = 0$, and the assertion is trivial. Otherwise, it follows from the Pythagorean theorem, because h_i is normal to E^Δ . \square

In other words, the squared distance of x to h_i is the power distance of x to the point p_i with weight w_i . We therefore have the following geometric relation:

Theorem 2 *For all values Δ , the sectional diagram $\mathcal{V}(H) \cap E^\Delta$ is identical to the power diagram of the points p_1, \dots, p_n , for the weights w_i in Lemma 1.*

In particular, if E^Δ lies below all tips then the Euclidean Voronoi diagram of p_1, \dots, p_n is obtained.

Figure 1 displays the trisector arcs of $\mathcal{V}(H)$ for a set H of 10 halflines. A corresponding sectional power diagram is shown in Figure 2.

Theorem 2 indicates that $\mathcal{V}(H)$ must have a relatively simple structure, which we will study now in more detail. First of all, the weights w_i , when seen as functions $w_i(\Delta)$, are continuous. $w_i(\Delta)$ is zero for $\Delta \leq z_i$, and decreases quadratically for $\Delta > z_i$.

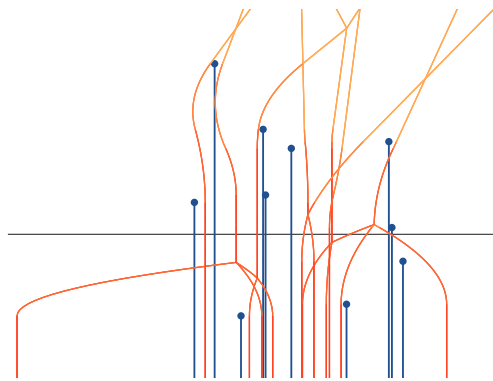


Figure 1: A halfline diagram with sectional plane, projected normal to the z -axis.

We watch the interplay on E^Δ when Δ is increased from $-\infty$ to ∞ . The power cells $C_i(\Delta) = \text{reg}(h_i) \cap E^\Delta$ are convex polygons, whose vertices move continuously. For sufficiently small Δ , each cell $C_i(\Delta)$ is a planar Voronoi region, and therefore is non-empty. Its edges first poise, and then move self-parallelly because p_1, \dots, p_n stay fixed, and movement is in a fixed direction by the shape of the bisectors B_{ij} . So each point $x \in E^\Delta$ can enter or leave $C_i(\Delta)$ at most once. Also, if $C_i(\Delta)$ disappears from the diagram it cannot reappear, by the monotone movement of its edges. We summarize:

Property 1 *The intersection of $\text{reg}(h_i)$ with every vertical line is connected or empty. Moreover, $\text{reg}(h_i)$ is a simply-connected set.*

Note that a power cell $C_i(\Delta)$ survives for $\Delta \rightarrow \infty$ if and only if the tip z_i appears on the upper convex hull of $\{h_1, \dots, h_n\}$. Property 1 does not imply that the combinatorial size of $\text{reg}(h_i)$ is $O(n)$: Although the number of bisectors B_{ij} that border $\text{reg}(h_i)$ is trivially limited to $n - 1$, a single bisector may define more than one *facet* (connected boundary patch) of $\text{reg}(h_i)$. Indeed, there are multiple adjacencies between the regions in $\mathcal{V}(H)$ in general; see Section 4.

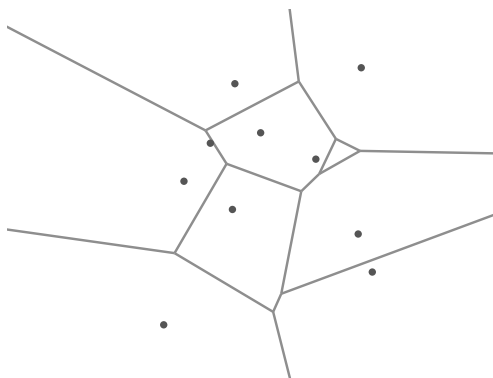


Figure 2: The sectional power diagram.

Let us now have a look at the Voronoi diagram $\mathcal{V}(\{h_i, h_j, h_k\})$ for only three halflines. The trisector curve t_{ijk} corresponds to a power diagram vertex $u^\Delta = t_{ijk} \cap E^\Delta$ for all Δ , unless the points p_i, p_j , and p_k are collinear (which we will exclude for the ease of description). This implies:

Property 2 *Each trisector t_{ijk} is a connected curve, unbounded in both z -directions, and monotone.*

In particular, t_{ijk} does not contain cycles. For pairwise different tip heights, the curve t_{ijk} is composed of 4 pieces, as can be easily verified: a halfline, two quadratic arcs, and another halfline. Therefore the algebraic degree of t_{ijk} is only two. Still, trisectors show a complicated intersection pattern in general. We will address this issue in Section 4.

3 Algorithm

Theorem 2 suggests a plane-sweep algorithm that computes the diagram $\mathcal{V}(H)$ in ascending z -direction.

The task is to maintain a power diagram for fixed points in the plane, under variation of their weights. The incidence structure of $\mathcal{V}(H)$ then can be inferred from the combinatorial changes that take place in the power diagram: When a power diagram edge appears (or disappears, respectively), then a facet of $\mathcal{V}(H)$ is born (or completed). Moreover, the collapse of a power cell signals the completion of a region in $\mathcal{V}(H)$.

An entirely two-dimensional implementation has been done, which avoids computing (costly) intersections of three-dimensional bisectors. Once the combinatorial structure of $\mathcal{V}(H)$ has been extracted, the bisector patches and trisector arcs that determine the geometry of $\mathcal{V}(H)$ are calculated in a final step.

To describe the combinatorial part of the algorithm in more detail, let $\text{PD}(\Delta)$ be the power diagram for the points p_1, \dots, p_n with weights $w_1(\Delta), \dots, w_n(\Delta)$, as defined in Section 2. We start with any value $\Delta < \min\{z_1, \dots, z_n\}$, and initialize $\text{PD}(\Delta)$ as the planar Voronoi diagram of $\{p_1, \dots, p_n\}$.

There is only one type of *events* (z -values) where the power diagram can change. These are the anticipated life ends a_{ij} of its edges e_{ij} .

More specifically, a_{ij} is the z -value of the lowest intersection point above E^Δ of the respective two trisector curves t_{ijk} and t_{ijm} , which define the endpoints of e_{ij} . This value can be calculated in $O(1)$ time, by solving a quadratic equation in z for each of the intervals given by z_i, z_j, z_k, z_m . In the diagram $\text{PD}(a_{ij})$, an update of constant complexity has to be performed. This update is either a flip that replaces the edge e_{ij} by the edge e_{km} (and a facet of $\mathcal{V}(H)$ in B_{ij} gets completed), or a collapse of a triangular cell incident to the edge e_{ij} , say $C_i(a_{ij})$ (and the region $\text{reg}(h_i)$ gets completed).

The tips z_i of the halflines h_i do not lead to combinatorial changes in $\text{PD}(z_i)$. They only alter the speeds of the edges in the power cell $C_i(z_i)$. This information is already incorporated in the trisector intersection task above.

We use a priority queue organized by z -values to maintain the order of events. Only $O(n)$ entries need to be stored at a time, by the linear number of edges in the power diagram $\text{PD}(\Delta)$. The next event to be performed then is accessible in $O(\log n)$ time. Moreover, the total number of entries a_{ij} is bounded by the number of facets of $\mathcal{V}(H)$.

Note finally that the numbers of facets, arcs, and nodes of $\mathcal{V}(H)$ are linearly related: A region with f facets has $O(f)$ arcs and nodes, because the degree of its nodes is at least 3. We conclude:

Theorem 3 *$\mathcal{V}(H)$ can be computed in logarithmic time per face, using $O(n)$ extra storage.*

4 Trisectors

The combinatorial size of $\mathcal{V}(H)$ tends to be near-linear for many data, as has been observed in our experiments. Thus the output-sensitive algorithm in Section 3 can be expected to run fast in practice. On the other hand, $\mathcal{V}(H)$ can attain a complexity of $\Omega(n^2)$, for example, when the tips z_i are arranged like in a worst-case example for the Voronoi diagram of point sites in \mathbb{R}^3 . This almost matches the upper bound of $O(n^{2+\varepsilon})$ for $\mathcal{V}(H)$, which follows from the more general bound in [10]; see Section 1. Proving a possible quadratic upper bound is complicated by the fact that the trisector curves of $\mathcal{V}(H)$ do not behave like pseudo-lines. Let us briefly comment on this fact.

For the halfline h_i with lowest tip, its region is always convex; all the bisectors B_{ij} either ‘bend’ towards h_i or are vertical planes. If the size of $\text{reg}(h_i)$ can be shown to be $O(n)$, then an insertion argument for regions in ascending order of tip heights implies an overall $O(n^2)$ diagram size. Unfortunately, the result in [11] on the linear size of surface envelopes does not apply, because two trisector curves can intersect in more than one point.

To see an example, consider four halflines h_1, h_2, h_3 , and h_4 arranged as is illustrated in Figure 3, from the top view (left) and from the front view (right). The two trisector curves t_{123} and t_{234} (and two others) concur in a point x , if and only if there exists a sphere centered at x that simultaneously touches all four halflines. There are two such spheres, a smaller one resting on the tip of the rightmost halfline, and bigger one passing through all four tips.¹

¹Thanks go to Peter Widmayer’s group for pointing us to this example.

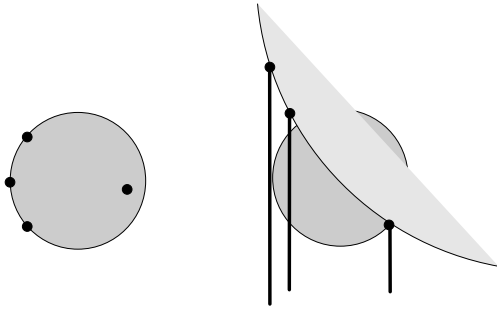


Figure 3: Two touching spheres for 4 halflines.

The trisectors defined by 4 halflines can have at most 3 intersection points, by a simple algebraic case analysis. This bound is actually attained, and even worse, there are constellations of n halflines for any $n \geq 4$ where every quadruple of related trisectors shows such an intersection behavior.

As another approach, one can try to bound the overall number of edges that appear in the power diagram $\text{PD}(\Delta)$ for varying Δ . There are $\binom{n}{2}$ potential power edges. However, once having disappeared, an edge between the same two power cells can appear again. In fact this can happen $n - 2$ times, which is the maximum possible. Stated differently, a fixed bisector B_{ij} can define $\Theta(n)$ facets where the two regions $\text{reg}(h_i)$ and $\text{reg}(h_j)$ are adjacent.

On the other hand, edge speeds in $\text{PD}(\Delta)$ are not arbitrary. Starting with 0, the speed of an edge increases at constant acceleration, until it stays constant forever.

By the relationship between power diagrams and convex hulls (see e.g. [5]), the problem above can be transformed into a dynamic convex hull problem in \mathbb{R}^3 . Starting from the paraboloid of revolution $z = x^2 + y^2$ at different times, n points move upwards vertically and at constant accelerations. The question of interest is now to bound the number of combinatorial changes that occur on their convex hull.

5 Extensions

An obvious extension of the results in this note concerns the Voronoi diagram of parallel line segments that are bounded in *both* directions. Whereas Lemma 1 can be generalized straightforwardly such that Theorem 2 still holds, the resulting plane-sweep algorithm now has to deal with the detection of new regions, which cannot be done locally. A simple solution is to calculate the respective Δ -values directly and beforehand, in $O(n \log n)$ time each.

Theorem 4 *The Voronoi diagram of n parallel line segments in \mathbb{R}^3 can be computed in $O((n^2 + K) \log n)$ time and optimal space, where K denotes the size of the output.*

Our results also generalize to higher dimensions. For example, for computing the Voronoi diagram of parallel line segments in \mathbb{R}^4 , a power diagram in \mathbb{R}^3 can be maintained. The sweep algorithm then constructs the desired diagram 2-face by 2-face and retains its output-sensitivity, though details get more involved.

References

- [1] I. Adamou. Curvas y superficies bisectrices y diagrama de Voronoi de una familia finita de semirrectas paralelas end R^3 . Ph.D. thesis, Department of Mathematics, University of Cantabria, Spain, 2013.
- [2] O. Aichholzer, W. Aigner, F. Aurenhammer, and B. Jüttler. Exact medial axis computation for triangulated solids with respect to piecewise linear metrics. *Proc. Curves and Surfaces 2011*, J.-D. Boissonat et al. (eds.), Springer Lecture Notes in Computer Science 6920, 2011, 1–27.
- [3] B. Aronov. A lower bound on Voronoi diagram complexity. *Information Processing Letters* 83 (2002), 183–185.
- [4] F. Aurenhammer and H. Imai. Geometric relations among Voronoi diagrams. *Geometriae Dedicata* 27 (1988), 65–75.
- [5] F. Aurenhammer, R. Klein, and D.T. Lee. *Voronoi diagrams and Delaunay Triangulations*. World Scientific, Singapore, 2013.
- [6] L.P. Chew, K. Kedem, M. Sharir, B. Tagansky, and E. Welzl. Voronoi diagrams of lines in 3-space under polyhedral convex distance functions. *Proc. 6th ACM-SIAM Symposium on Discrete Algorithms*, 1995, 197–204.
- [7] I. Emiris, T. Malamatos, and E. Tsigaridas. Approximate nearest neighbor queries among parallel segments. *Proc. 26th European Workshop on Computational Geometry*, 2010.
- [8] H. Everett, D. Lazard, S. Lazard, and M. Safey El Din. The Voronoi diagram of three lines in R^3 . *Proc. 23rd Ann. Symposium on Computational Geometry*, 2007, 255–264.
- [9] V. Koltun and M. Sharir. Polyhedral Voronoi diagrams of polyhedra in three dimensions. *Discrete & Computational Geometry* 31 (2002), 83–124.
- [10] V. Koltun and M. Sharir. Three-dimensional Euclidean Voronoi diagrams of lines with a fixed number of orientations. *SIAM Journal on Computing* 32 (2003), 616–642.
- [11] J. Schwartz and M. Sharir. On the two-dimensional Davenport-Schinzel problem. *Journal of Symbolic Computation* 10 (1990), 371–393.
- [12] M. Sharir. Almost tight upper bounds for lower envelopes in higher dimensions. *Discrete & Computational Geometry* 12 (1994), 327–345.